15. PHYSICAL PROPERTIES SYNTHESIS, LEG 20, DEEP SEA DRILLING PROJECT

George Z. Forristall, Shell Development Company, Houston, Texas

Although a synthesis of the physical properties data collected during this cruise did not yield any startling results, it did permit a general discussion of several interesting problems. The Leg 20 data are presented mainly on scatter diagrams that display the variation of one physical property with respect to another. In many cases these diagrams are aptly named, but in others definite correlations are evident. Once the data from the site summaries are collected on punch cards, it is a simple matter for a computer to produce graphs of the variables in any conceivable combinations, which may than be studied for possible significant features. Those which seemed worthy of some note are displayed here.

The first and most obvious correlation to check is systematic variation of physical properties with depth below the mud line. Figures 1 and 2, for example, show porosity and sonic compressional velocity versus depth of burial. In this and subsequent figures, all measurements on indurated samples are shown, along with a representative measurement for each core barrel of unconsolidated material. In both figures, points seem almost randomly scattered. This perhaps should not be too surprising considering the variety of depositional environments encountered at the various sites. However, even at individual sites, chalk-chert sequences consist of materials with vastly different physical properties in juxtaposition. The most we can probably say is that maximum porosity decreases with depth, and minimum sonic velocity increases slightly with depth.

The dotted line in Figure 2 is based on studies by Laughton (1954) of artificially compacted globigerina ooze and should be a rough lower limit to the velocities possible in the natural environment. Unfortunately, many of the measured points are decidedly below this line. Furthermore, the Leg 20 sonobuoy refraction measurements reported by Jones (this volume) give significantly higher velocities in the upper transparent layer than those measured in the shipboard laboratory for Sites 194 and 195. Such discrepancies can easily be ascribed to the obvious disturbance of the samples by the drilling process, but it is likely that a more basic problem exists; namely, that to mimic conditions in buried sediment the material must be artificially compacted. Many theoretical and experimental studies such as those by Biot (1956) and Birch (1960) have shown that for a porous material, sound velocity increases with effective pressure in the same manner shown by the dotted line in Figure 2. It is important to think in terms of effective pressure since the fluid pressure is also felt in the pores between the grains, and essentially only the weight of overburden results in compaction. Since the samples are tested at atmospheric pressure in the laboratory, it is obvious that their velocities will be lower than those of in situ materials. With these considerations, the surprising fact is that the sonobuoy measurements at Site 199 match the laboratory measurements. A possible, but not too convincing, explanation is the thinness of the upper transparent layer at that site.

Other scatter patterns are easier to explain. The density-porosity plot of Figure 3 shows a straight line correlation which resulted from using the densities of calculate porosities. The dotted line shows the expected values for a grain matrix density of 2.68, and all the grain matrix densities assumed for the samples were near this value.

The relationship between porosity and velocity or density and velocity is of some practical importance, since porosity and density are easier to measure, but sonic velocity is more useful. Figures 4 and 5 show these relationships based on our data. The dotted lines in the figures are plotted from semiempirical equations which Nafe and Drake (1957; 1963) found to fit experimental data from a wide range of sources. The trend of our sample points is generally higher than the curve, particularly near a porosity of 0.5. An explanation may lie in the fact that most of Nafe and Drake's data in this range came from artificially compacted oozes, whereas most of our come from partly indurated material. Higher velocities would be expected through cemented grains than through merely compacted grains.

Whenever possible, sonic velocities were measured both parallel and perpendicular to the bedding plane. Figure 6, in which the abscissa is the compressional velocity across the bedding plane and the ordinate the velocity parallel to the bedding plane, shows the results for all samples on which both measurements were made. The dotted line shows the expected value for an isotropic material. The measured values are consistently above the line; that is, the velocity was usually higher parallel to the bedding plane, though only by a few percent. This could be another reason for the refraction measurements giving higher velocities than the laboratory measurements, although samples from the upper transparent layer were isotropic by the time they reached the laboratory.

For heat flow studies, it is desirable to have a relationship between thermal conductivity and some more commonly measured property. Figure 7 shows thermal conductivity versus porosity for Leg 20 samples. The points, which are unfortunately few, show the inverse correlation noted by Langseth and Von Herzen (1971).

Triaxial tests on some indurated samples collected during Leg 20 are reported in this volume by Smith and Forristall. It is interesting to see if there is any relationship between the mechanical properties and the physical properties customarily measured. Figure 8 shows an inverse correlation between porosity and failure strength at 10,000 psi confining pressure, and Figure 9 shows a direct correlation between compressive velocity and yield strength

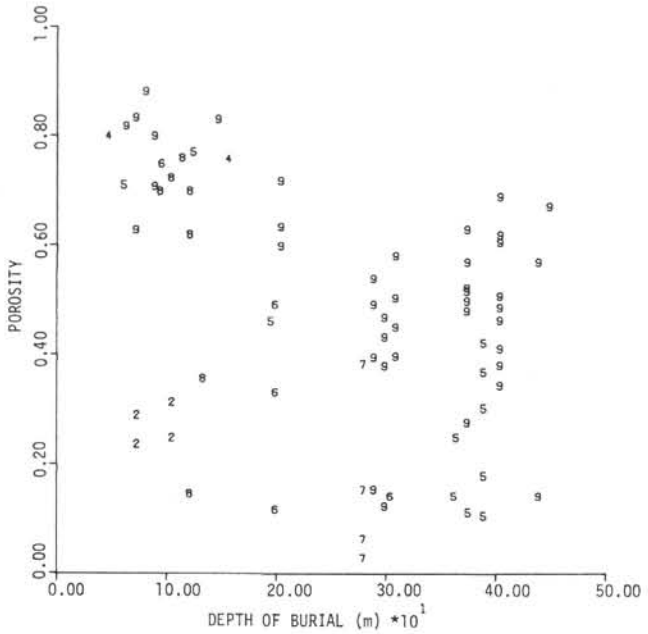

Figure 1. *Porosity vs. depth at Leg 20 sites. Each plotted number is the last digit of the site from which the measurement was taken and is centered on the point that it represents.*

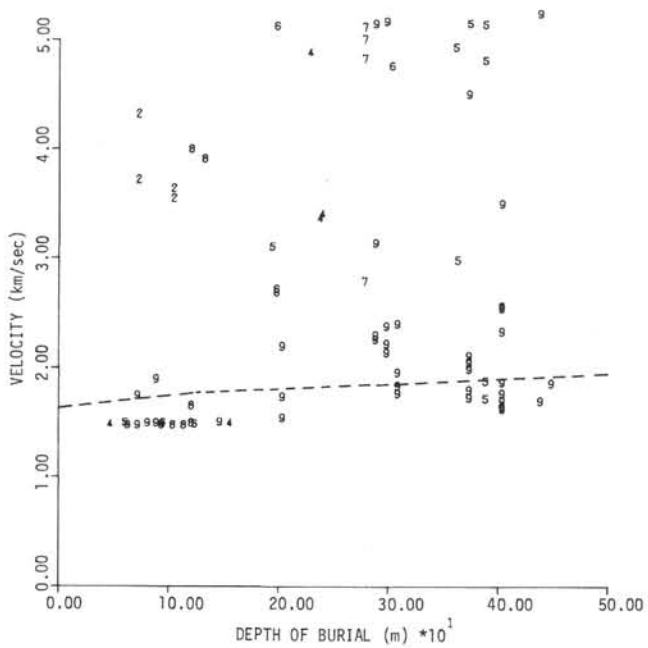

Figure 2. *Sonic compressional velocity vs. depth. Dashed line based on artificially compacted globigerina ooze (Laughton, 1954).*

at 10,000 psi confining pressure. Figure 10 shows the relationship between failure and yield strengths. These trends are interesting, though not unexpected, but since the data points are few and scattered, little more can be said.

It is often more useful to describe the strength of a material by the parameters of its Mohr envelope than by its

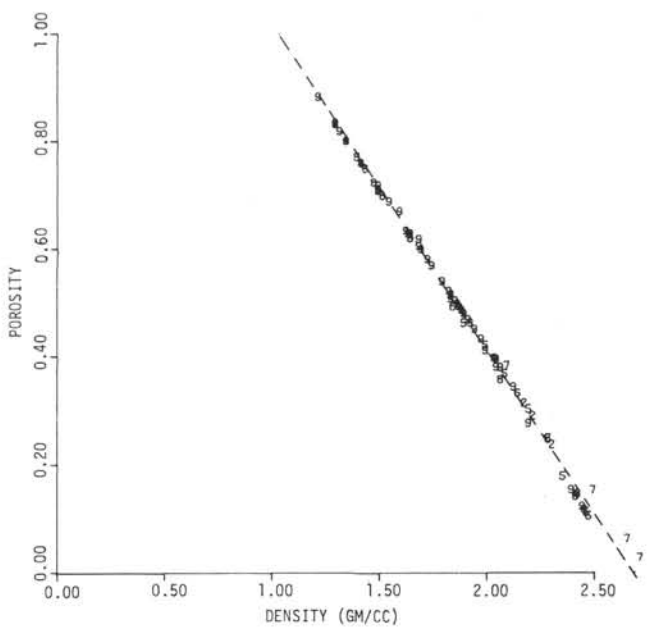

Figure 3. *Porosity vs. density. Dotted line represents expected values for grain matrix density of 2.68.*

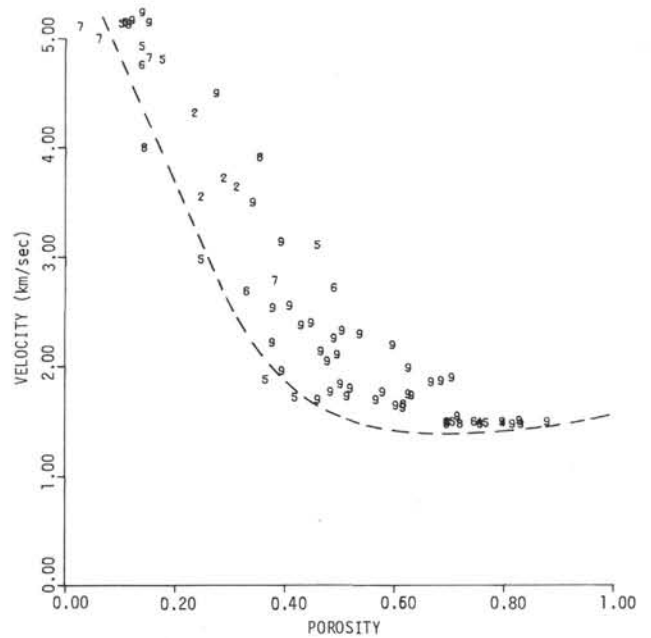

Figure 4. *Velocity vs. porosity for Leg 20 sites. Dashed line from semi-empirical determinations of Nafe and Drake (1957, 1963).*

strength at a particular confining pressure, since the Mohr envelope encloses the strengths for all pressures. Many Mohr envelopes can be approximated reasonably accurately by a straight line described by two parameters such that

$$\sigma_1 = \tau_o + \sigma_3 \tan \phi$$

where σ_3 is the confining pressure, σ_1 is the failure strength, and τ_o and ϕ are constants known as the

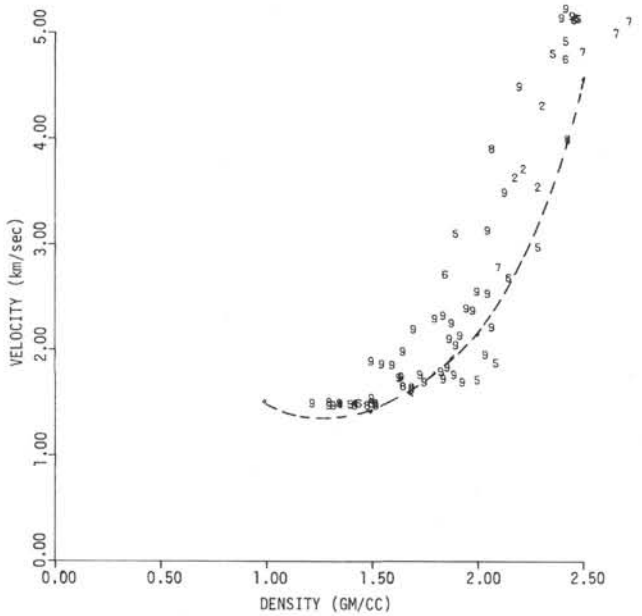

Figure 5. *Velocity vs. density for Leg 20 sites. Dashed line from semi-empirical determinations of Nafe and Drake (1957, 1963).*

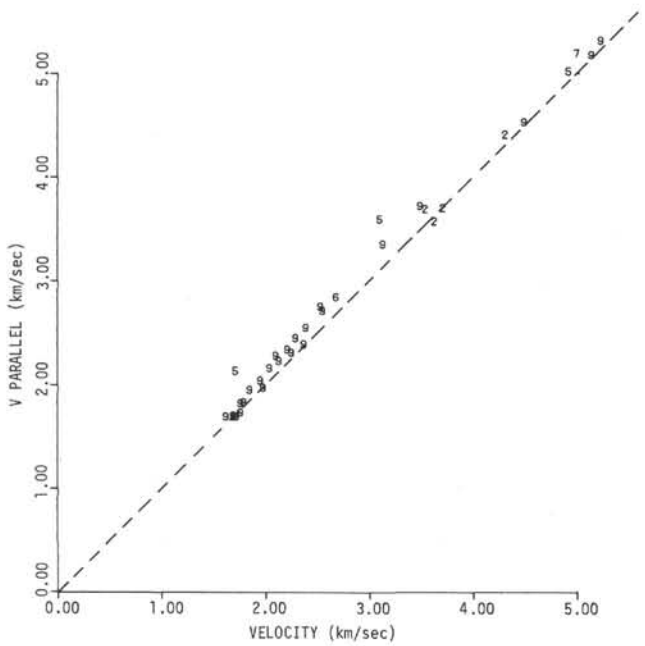

Figure 6. *Compressional sonic velocity parallel to bedding vs. compressional sonic velocity perpendicular to bedding for Leg 20 sites. Dashed line is that for isotopic material.*

unconfined shear strength and angle of internal friction, respectively. For each of the samples for which Smith and Forristall give failure strengths at two or more confining pressures tau and phi were determined, and plotted in scatter diagrams. There is little data and the results are inconclusive, but two examples, phi versus compressional velocity and tan versus porosity, are shown in Figures 11 and 12. The only conclusion is that there is some trend of increasing angle of internal friction with increasing velocity.

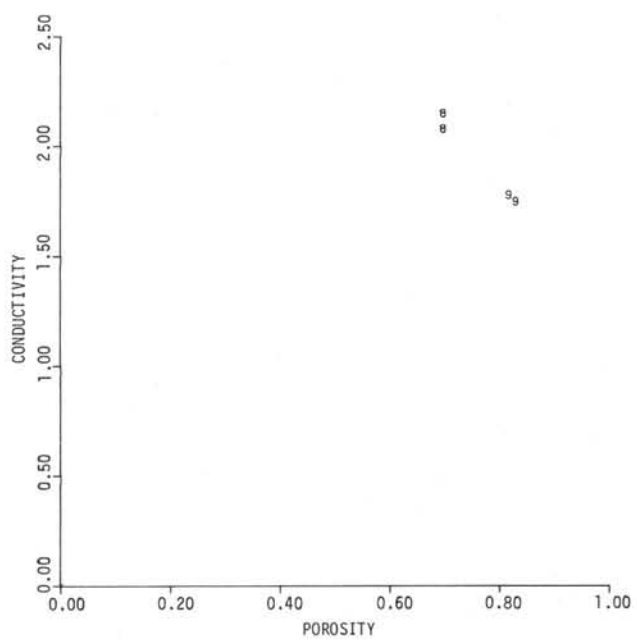

Figure 7. *Thermal conductivity vs. porosity for Leg 20 sites.*

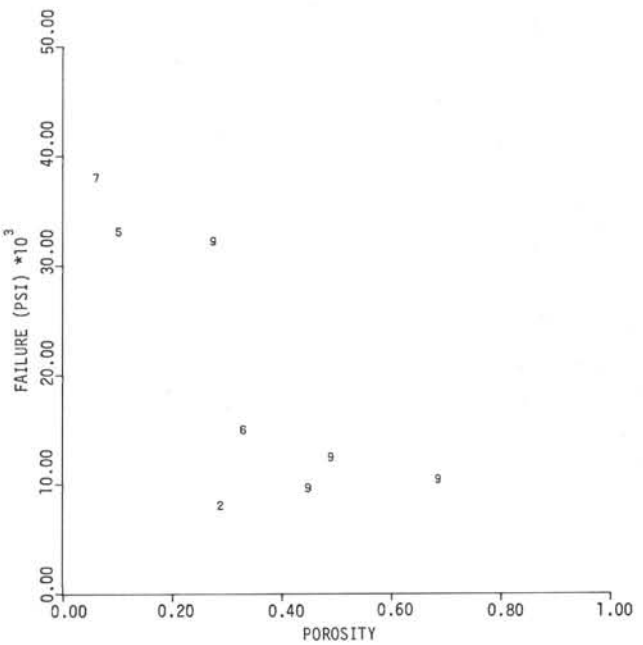

Figure 8. *Failure strength vs. porosity at 10,000 lbs. confining pressure, Leg 20 sites (see also Smith and Forristall, this volume).*

REFERENCES

Biot, M. A., 1956. Theory of propagation of elastic waves in a fluid saturated porous solid: J. Acoust. Soc. Am., v. 28, p. 168-191.

Birch, F., 1960. The velocity of compressional waves in rocks to 10 kilobars: J. Geophys. Res., v. 65, p. 1083.

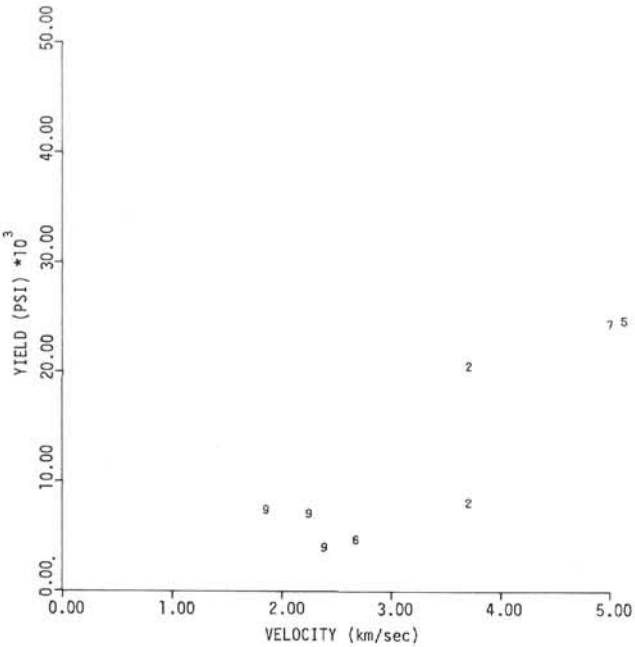

Figure 9. *Yield strength vs. compressive sonic velocity at 10,000 lbs. confining pressure, Leg 20 sites (see also Smith and Forristall, this volume).*

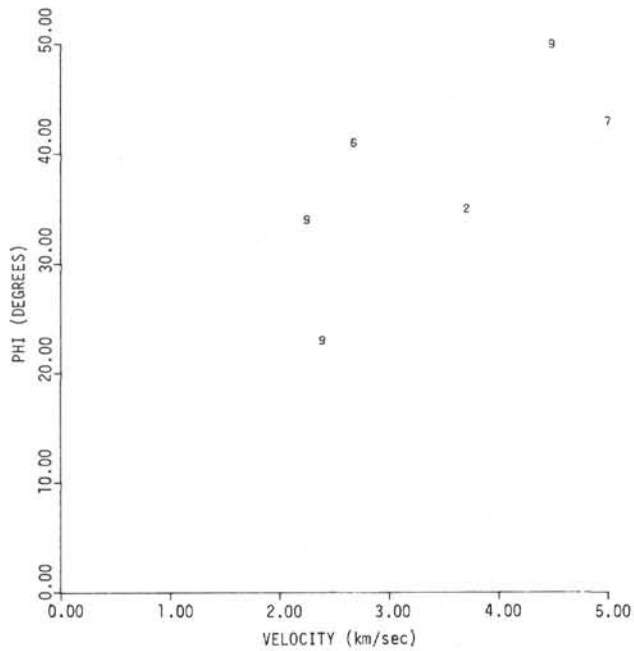

Figure 11. *Angle of internal friction vs. compressional sonic velocity, Leg 20 sites.*

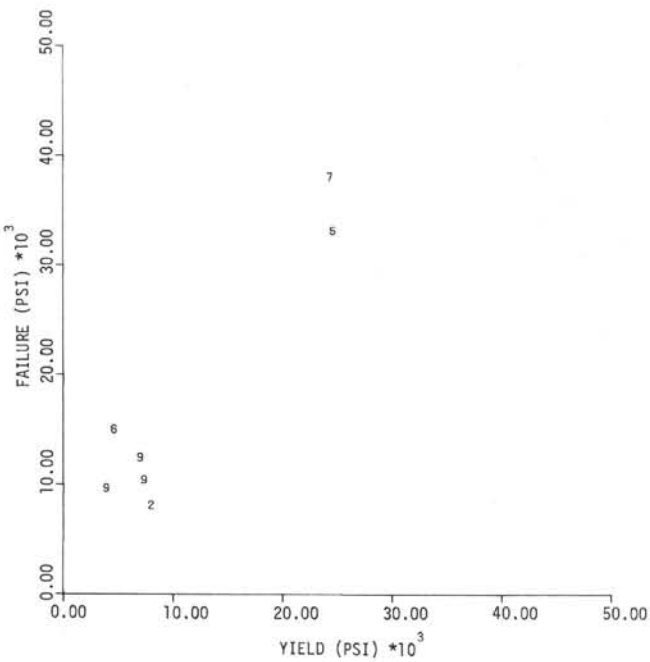

Figure 10. *Failure strength vs. yield strength, Leg 20 sites (see also Smith and Forristall, this volume).*

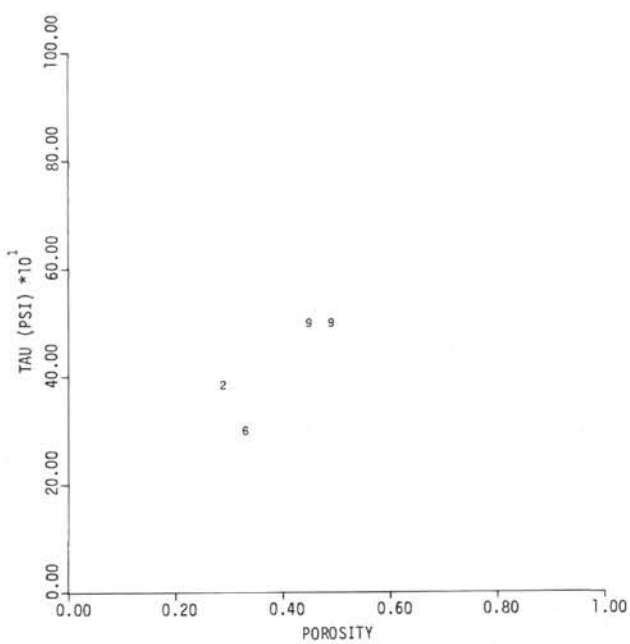

Figure 12. *Unconfined shear strength vs. porosity, Leg 20 sites.*

Langseth, M. G. and Von Herzen, R. P., 1970. Heat flow through the floor of the world oceans. *In* The sea: Vol. 4, Maxwell, A. E. (ed.), New York (Interscience), p. 299-353.

Laughton, A. S., 1954. Laboratory measurements of seismic velocity in ocean sediments. Roy. Soc. London, Proc., v. A222, p. 336-341.

Nafe, V. E. and Drake, C. L., 1956. Variation with depth in shallow and deep water marine sediments of porosity, density, and the velocities of compressional and shear waves: Geophysics, p. 523-552.

_____, 1963. Phsyical properties of marine sediments. *In* The sea;: Vol. 3, Hill, M. N. (Ed.), New York (Interscience), p. 794-815.